

Estimation of Weld Quality in High-Frequency Electric Resistance Welding with Image Processing

An image analysis algorithm can estimate the weld quality by using the weld image data during high-frequency electric resistance welding

BY D. KIM, T. KIM, Y. W. PARK, K. SUNG, M. KANG, C. KIM, C. LEE, AND S. RHEE

ABSTRACT. In high-frequency electric resistance welding (HF-ERW), the weld quality is determined by the welding phenomenon in the welding spot proximity. Methods to eliminate or minimize defects, therefore, include real-time monitoring of the weld quality and problem solving as problems arise. It is possible to estimate weld quality qualitatively by using the weld image data during HF-ERW. A method to predict the weld quality using image processing in the heating process of the HF-ERW point is proposed. An algorithm, which predicts the weld quality by using a vision sensor to obtain the image of the welding spot proximity thus best expressing the welding phenomenon, is developed. The heated area, which shows the image data with the highest correlation to the weld quality and the smallest amount of noise, is consequently calculated.

Introduction

In high-frequency electric resistance welding (HF-ERW), a high-frequency current in the range of 300~1000 kHz is applied to the welding area, and squeeze force is added to the workpiece heated from the heat resistance. The HF-ERW method is classified into the high-frequency induction method and the high-frequency resistance welding method, depending on the method employed in the application of high-frequency current on the workpiece. In the high-frequency in-

duction welding method, an induction coil is used in inducing high-frequency current to generate heat. In high-frequency resistance welding, on the contrary, a contactor is applied to the workpiece to directly provide the current (Ref. 1). High-frequency induction welding is primarily used in joining small-diameter steel pipes, while HF-ERW is used in joining large-diameter steel pipes.

The characteristic of HF-ERW is the resistance generated through the use of high-frequency currents dissimilar from direct or low-frequency currents. In high-frequency electric welding, the resistance heat is concentrated on the welding surface due to the skin effect wherein the current is concentrated on the conductor surface on account of the high frequency, and the proximity effect wherein the current is concentrated on the surface of two conductors as they approach each other. The area affected by heat can, therefore, be decreased and the welding speed can be increased, producing a welding method with superior productivity over the preceding methods.

Figure 1 shows an example of the direct contact method. The current is concentrated on the surface of each side of the pipe due to the skin and proximity effects when a high-frequency current is applied to the workpiece through a contactor. The resistance heat generated by the current causes partial melting, and the melting

surface is compressed by the squeeze roller, excreting oxidized material from the melting surface to generate a weld. The molten part of the pipe generated by the resistance heat contains oxidized material on account of exposure to the air. Therefore, if the oxidized material is not completely excreted during compression, and oxidized material remains in the welding part as an impurity, the weld quality becomes degraded.

Haga (Ref. 2) used a high-speed camera to observe the melting and joining mechanism around the V-convergence point. It was found that even when mechanic pressure was not applied to each section, the molten metal is excreted with the oxidized material due to the electromagnetic force. Also, the HF-ERW phenomenon is classified into three types according to the length and shape of the narrow gap. The first type of welding phenomenon is generated under low heat input conditions when the approach speed exceeds the melting speed, a narrow gap is not formed, and the welding point is formed near the V-convergence point. The second type of welding phenomenon is generated under optimal heat input conditions when the melting speed is equal to the approach speed, the gap is generated, and the welding point is formed at the end of the narrow gap thus producing the most favorable weld. The third type of welding phenomenon is generated under high heat input conditions when the melting speed exceeds the approach speed, the gap is too large, and a momentary short circuit occurs before the welding point is formed.

Haga (Ref. 3) has categorized weld defects into cold weld and penetrator. The cold weld is a defect generated during the first type of welding phenomenon when the welding heat input is smaller than the optimal heat input, while the penetrator is a defect generated during the third type of welding phenomenon when the welding heat input is larger than the optimal heat

D. KIM is with Joining & Coating Technology, Shipbuilding & Plant R & D Institute, Samsung Heavy Industries Co., Geoje-si, Korea. T. KIM, Y. W. PARK, K. SUNG, and S. RHEE are with the Department of Mechanical Engineering, Hanyang University, Seoul, Korea. M. KANG is with Advanced Welding & Joining Research Team, KITECH Incheon, Korea. C. KIM is with Joining Research Group, POSCO, Pohang, Korea. C. LEE is with the Department of Mechanical Engineering, Seoul National University of Technology, Seoul, Korea.

KEYWORDS

High-Frequency Electric Resistance Welding (HF-ERW)
Weld Quality
Image Processing
Heated Width
Heated Area

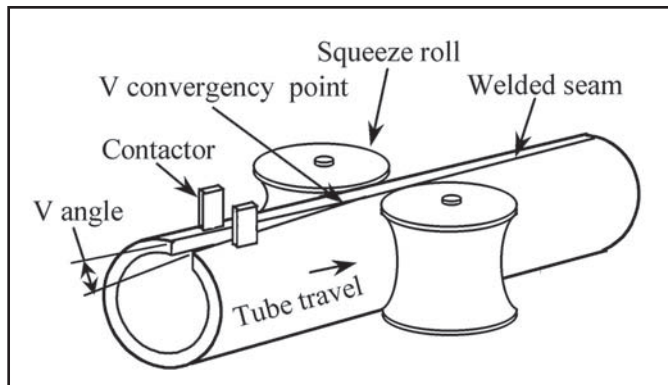


Fig. 1 — Schematic diagram of high-frequency electric resistance welding system.

input. External variables frequently affect the weld quality even when welding conditions are preset and welding is performed to produce favorable weld quality without defects. Real-time monitoring and control of the welding process, thus, are necessary in order to prevent weld defects and efficiently manage the production procedure. Based upon the results of Haga's research (Ref. 3) identifying the least weld defects in the second type of welding phenomenon and the most weld defects in the heat input conditions of the first and third types of welding phenomena, Watanabe et al. (Ref. 4) have used the correlation between the three types of welding phenomena found in HF-ERW and the frequency of the welding currents to monitor the welding frequency and to control the heat input in welding.

Mihara et al. (Ref. 5) have used a one-dimensional photodiode to calculate the heated width of the welding part to control the heat input, where the photodiode is set to calculate the welding part 30 mm behind the V-convergence point. The heated width of the welding part is calculated, and a feedback control system is established to maintain the value at a constant level. This method, however, retains a problem that the changing V-convergence point according to the welding conditions is excluded from consideration, and heated width calculated from a single point shows a high level of change according to the time thus undermining the correlation with the actual weld quality. In addition, the weld quality is determined by the welding mechanism near the welding point rather than the melting phenomenon behind the welding point in HF-ERW. The data calculated behind the welding point are, therefore, not closely correlated to the weld quality. Tatsuwaki et al. (Ref. 6) have formulated a system using a two-dimensional pattern thermometer to control the heat input by calculating the two-dimensional temperature distribution of the welding part. A two-dimensional tem-

perature sensor is used in this study to calculate and monitor the two-dimensional temperature distribution near the V-convergence point. The data controlling the heat input in this method, however, use the temperature distribution from only a particular line, and thus the method does not present a solution to overcome the shortcomings found in the studies of Mihara et al. (Ref. 5).

To date, the research results regarding high-frequency resistance welding have shown that the electric resistance welding (ERW) weld quality is closely correlated with the melting phenomenon caused by the resistance heat near the welding point. The data calculated from the welding phenomenon of ERW, however, are not highly reliable, and the ERW welding phenomenon, furthermore, fails to actively respond to the changing V-convergence point. In order to overcome such problems in this study, active responses are made to the changing V-convergence point in HF-ERW, and a welding phenomenon value highly correlated to the weld quality is obtained with a method to estimate the real time weld quality proposed. Electric resistance welding image data taken with a high-speed camera are used in this study in order to develop an algorithm, which obtains and calculates data showing the highest correlation between the weld quality and welding phenomenon.

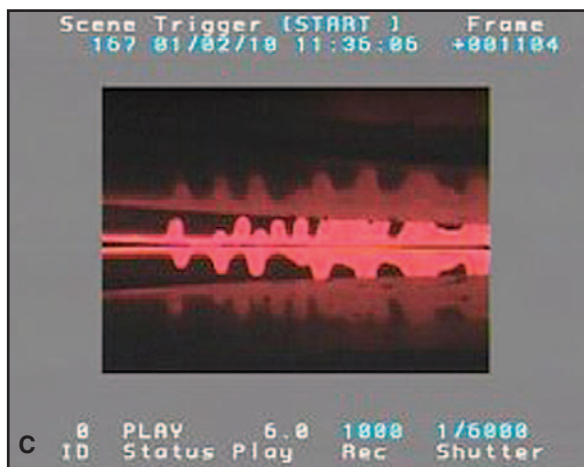
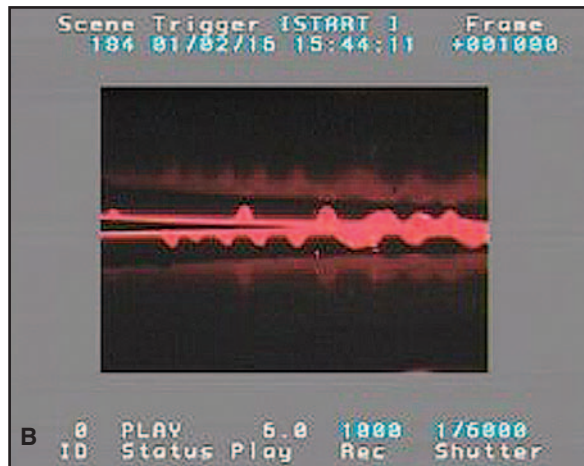


Fig. 2 — Image of welding phenomena captured by a high-speed camera. A — Low heat input; B — optimal heat input; and C — high heat input.

Raw Image Acquisition System

A high-speed camera was used in order to observe the melting phenomenon in HF-ERW with the filming speed set at 1000 fps to capture the welding phenomenon around the V-convergence point. The thickness of the base metal was 10 mm,

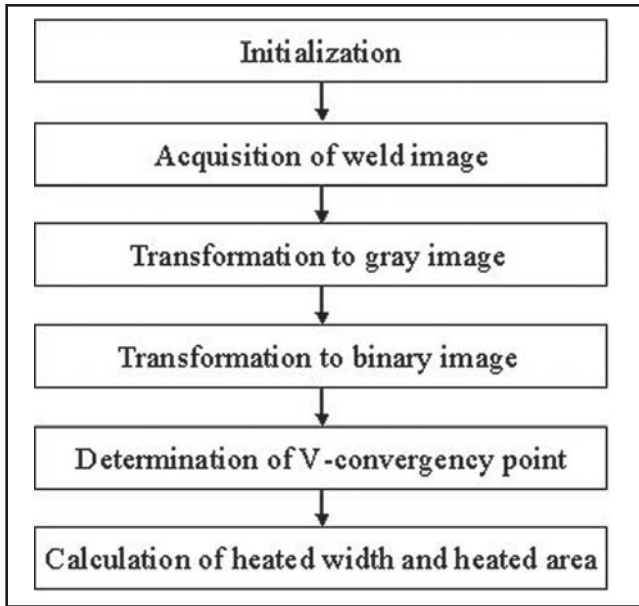


Fig. 3 — Image processing procedures.

and the chemical composition of the base metal was shown in Table 1.

The main welding variables affecting the weld quality in HF-ERW were determined to be the V angle, welding speed, welding power, squeeze force, and current frequency. In this study, the squeeze force was fixed at a constant value and the current frequency was set at 310 kHz, while the V angle, welding speed, and welding power were changed during filming. The analog images taken through the high-speed camera under each welding condition were converted and stored as digital color images of 720(H)*480(V) pixels. The high-speed ERW phenomenon was analyzed and the results were used to extract the parameters related to the weld quality.

Figure 2 shows three examples of the images taken with the high-speed camera. According to the categorization by Haga (Ref. 2), Fig. 2A shows the first type of welding phenomenon, while Fig. 2B shows the second, and Fig. 2C shows the third type. Figure 2A–C, in addition, shows that the V-convergence point moves forward as the heat input increases. X-ray and ultrasonic tests for test pieces of the three images show the following results. Figure 2A is an image of a weld defect under low heat input, while Fig. 2C is an image of a weld defect caused by excess heat input such as a penetrator. No defects can be found in Fig. 2B, which shows welding conditions with optimal heat input. By using the image data of the welding part in Fig. 2, it becomes possible to produce a qualitative estimate of the weld quality. An image analysis algorithm producing a quantitative estimate of the qualitative estimate

above is required in order to formulate a system, which can monitor the real time welding phenomenon.

Image Processing Procedures

In a weld quality estimation system using HF-ERW image data, the level of fluctuation in the weld quality parameters must be small under identical welding conditions as long as the parameters have a high correlation to the weld quality with external noise nonexistent. An image analysis is conducted in this study in order to extract

the weld quality parameters from the image data obtained through a high-speed camera. The image analysis is performed using the heated width suggested

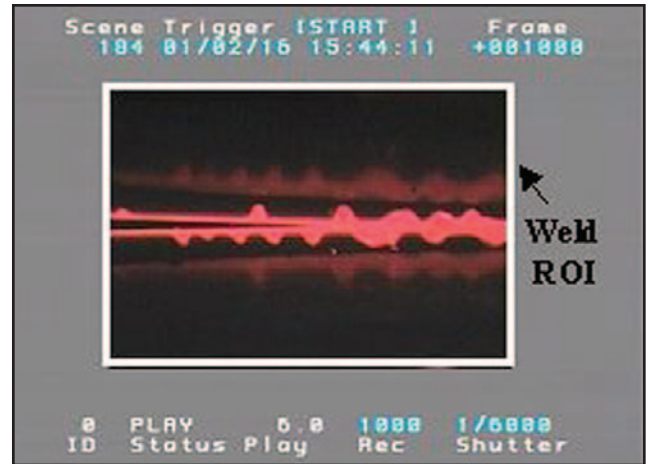


Fig. 4 — Region of interest of an ERW phenomenon.

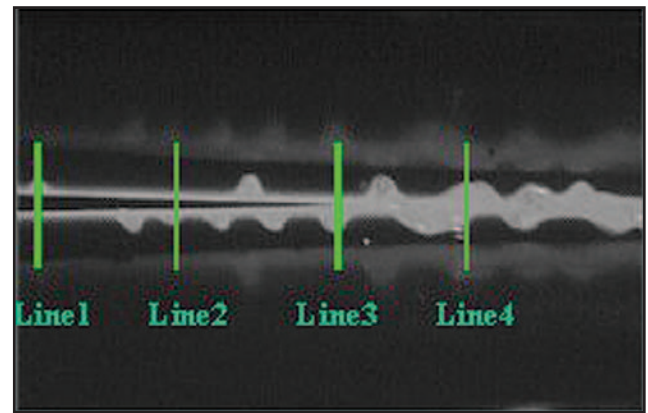


Fig. 5 — Gray image of an ERW phenomenon.

Table 1 — Chemical Composition of Base Metal (wt-%)

C	Si	Mn	P	Cr	Al	Cu	Nb	V
0.062	0.194	1.32	0.015	0.012	0.031	0.018	0.023	0.027

Table 2 — The Coefficients of Variation for Image Data Sampled per 0.1 s

Items		Welding power				
		202 kW	216 kW	230 kW	244 kW	258 kW
Heated width	Line 1	32.48	31.51	30.48	37.17	24.85
	Line 2	35.39	37.15	29.24	39.26	42.14
	Line 3	19.05	35.78	15.65	28.80	11.71
	Line 4	27.64	30.06	13.77	23.45	21.68
Heated area		2.88	2.96	3.26	3.17	3.68

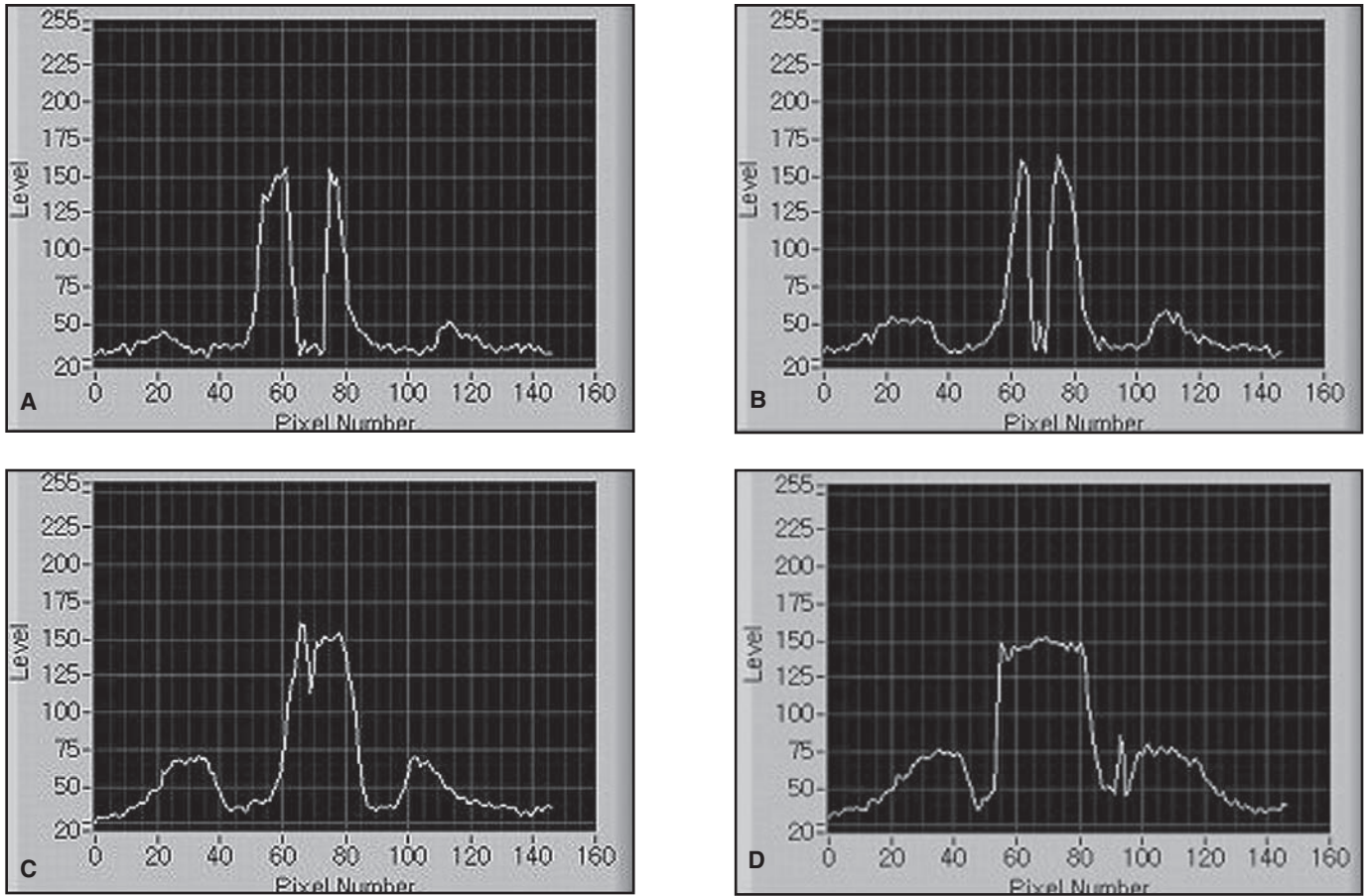


Fig. 6 — Line profiles of the gray image. A — profile of line 1; B — Profile of line 2; C — profile of line 3; and D — profile of line 4.

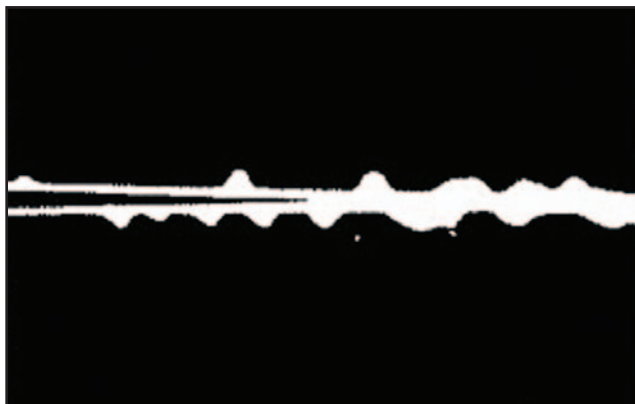


Fig. 7 — Converted binary image.

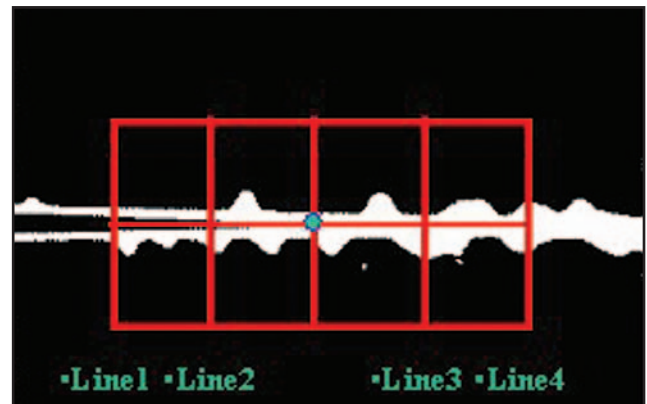


Fig. 8 — Region of interest for calculating heated width and heated area.

in the previous study and the heated area suggested in this study as parameters. The changes in the V-convergence point according to the V angle and heat input during welding are taken into consideration, and thus the heated width and heated area are calculated based upon the V-convergence point in order to reduce changes in weld quality parameters

induced by the changes in the V-convergence point.

Figure 3 shows the image processing procedure for each frame. Four factors including the region of interest (ROI), the threshold value of the gray level to determine the heated area of the image, the location where the heated area is to be measured, and the location where the heated

width is to be measured are determined in order to analyze the image in the first stage of initialization. In the second stage, the image signal obtained through the high-speed camera is transferred into a digital image. Figure 4 shows an image converted into a digital image. The size of the image is 720(H)*480(V) pixels, and the area to be welded is marked by the

weld ROI showing an area of 436(H)*282(V) pixels. The corresponding ROI of the actual welding part is 60(H)*39(V) mm, and thus an algorithm is formulated to perform the actual image processing only on the ROI.

In the third stage, the color image is converted into a gray image. Figure 5 shows an image wherein the ROI has been converted into gray level (0~255). The more intense the heat caused by the heat resistance, the higher the gray level. This shows a shade closer to white as shown in the figure.

In the fourth stage, the line profile of the gray image is used to determine the threshold value, and the areas below the threshold value are considered 0 with the heated areas exceeding the threshold value being considered 255. Figure 6 shows the gray level of each point within the four lines marked in Fig. 5. It is necessary to select a threshold value, which does not influence the heated width or the heated area to the highest degree by cooling water and other disturbance factors. In this paper, gray level of 110 was selected as the threshold value based on Fig. 6. Fig-

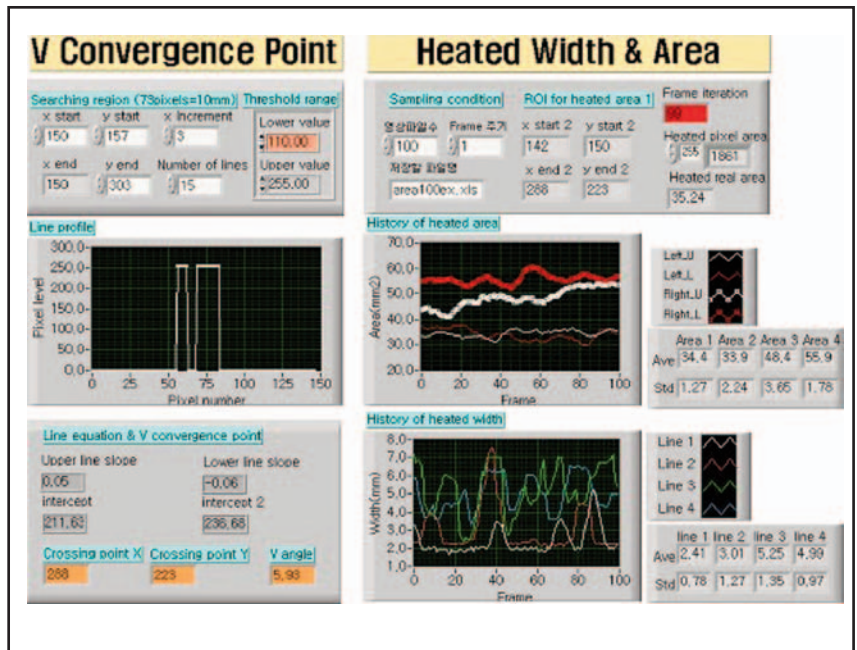


Fig. 9 — LabVIEW front panel for calculating weld quality parameters.

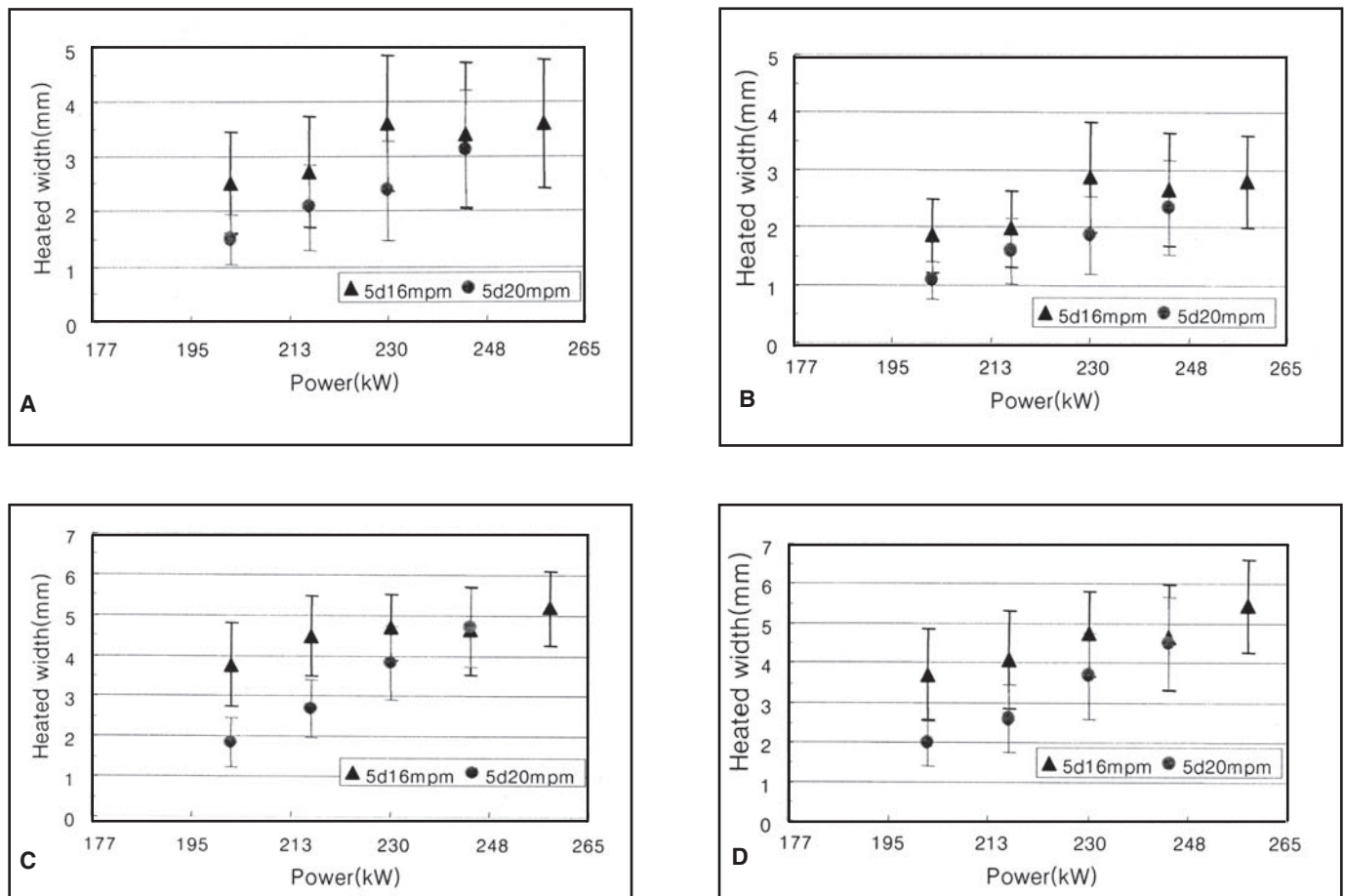


Fig. 10 — Heated width from images captured per 0.001 s. A — Line 1; B — line 2; C — line 3; and D — line 4.

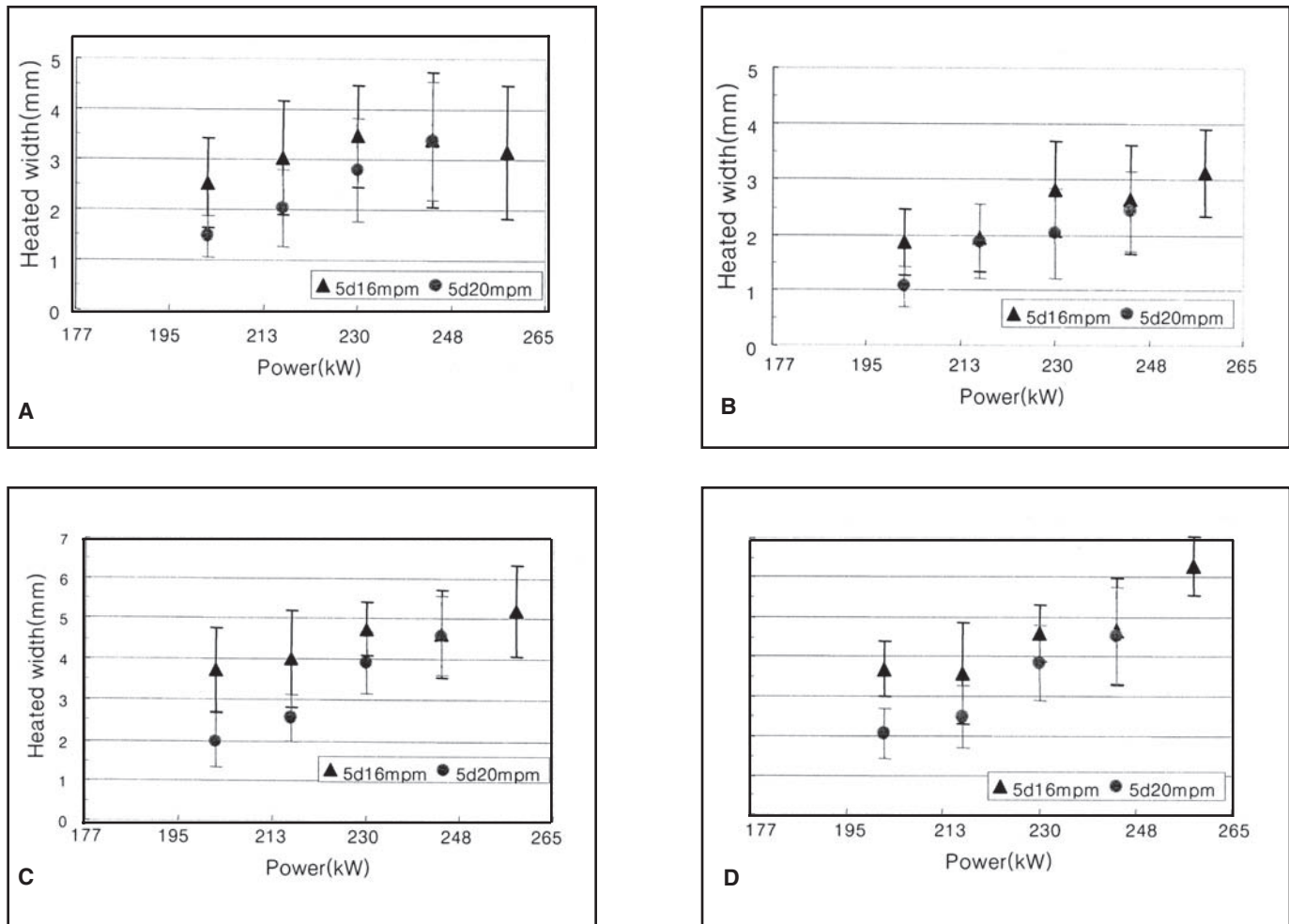


Fig. 11 — Heated width from images captured per 0.1 s. A — Line 1; B — line 2; C — line 3; and D — line 4.

ure 7 shows the image converted into a binary image after determining the threshold value at 110. The gray level of areas below 110 is considered 0, and the gray level of areas exceeding 110 is considered 255. Hence the white areas in the figure show the heated area.

In the fifth stage, the V-convergence point is obtained from the binary image. The V-convergence point is calculated after detecting the two lines comprising the V angle. The gray level values of each row are searched within the binary image data, which are stored in the matrix form. The set of points where the gray level value has been converted from 255 to 0 and a set of points where the gray level has been converted from 0 to 255 are extracted, and the least square method is applied to each set to obtain the two line equations. The two line equations are consequently used to determine the V angle and the coordinates of the V-convergence point.

In the final stage, the V-convergence point obtained in stage 5 is used to calculate the heated width and area. Figure 8

shows the location within the image where the heated area and heated width are measured. The heated width is measured at four points in 10-mm intervals from the V-convergence point, while the heated area is calculated by searching the area 10 mm above and below the V-convergence point and 20 mm to each side. The points wherein the gray level is 255 are extracted within the area to measure the heated area.

Result and Discussion

In order to induce a correlation between the narrow gap and the welding quality, Haga (Ref. 2) has measured the narrow gap in the welding part in an image of the welding phenomenon. The narrow gap can, however, only be observed through a high-speed camera. Hence, the narrow gap cannot be observed through a standard 30-fps camera, and the measurement continually changes even under identical welding conditions, making it difficult to monitor and control the narrow gap. It is necessary to select factors re-

taining a high correlation with the welding quality when determining the factors for welding quality monitoring, and to show a minimum level of fluctuation under identical welding conditions when external noise is nonexistent. In this study, LabVIEW (Ref. 7) is used for image analysis, and Fig. 9 shows the front panel composed through LabVIEW. The front panel shows weld image parameters such as V-convergence point, heated area, etc. Images of the welding phenomenon are taken while differing the welding power under a 5-deg V angle and welding speed at 60 and 20 m/min. In addition, image processing is conducted with a sampling interval of not only 0.001 s, but also 0.1 s in order to observe the possibility of monitoring the welding phenomenon using a standard 30-fps CCD camera, which is far more cost efficient than a high-speed camera. The number of samples acquired in the sampling interval of 0.001 s is 1500, while 15 samples are obtained when the sampling interval is set at 0.1 s.

Figure 10 shows the heated width mea-

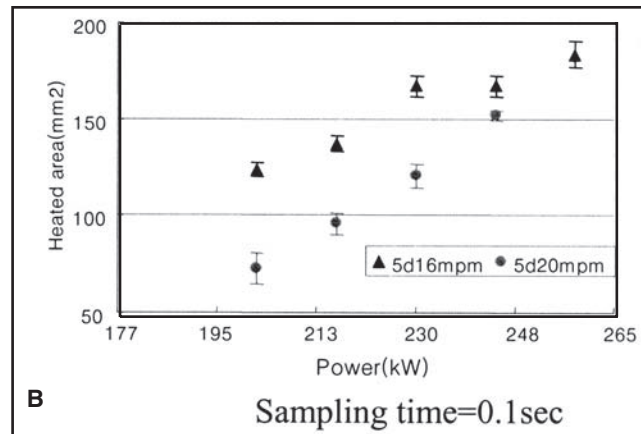
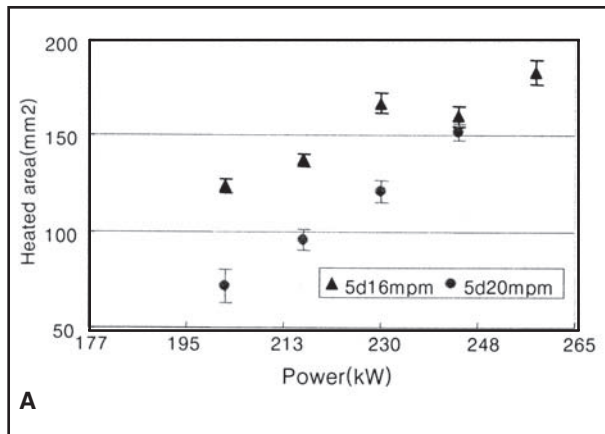


Fig. 12 — Heated area from images captured per 0.001 and 0.1 s. A — Sampling time = 0.001 s; and B — sampling time = 0.1 s.

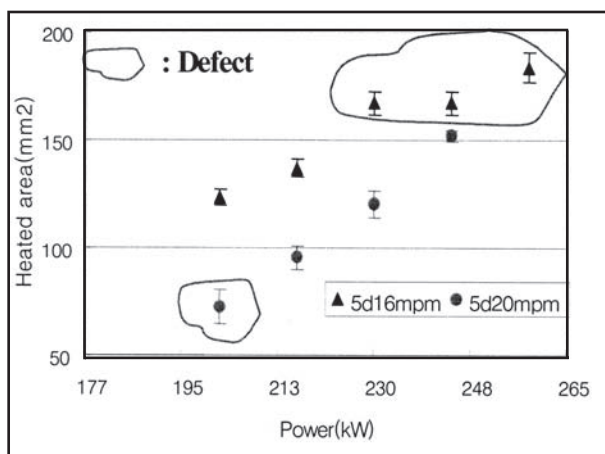


Fig. 13 — Relationship between weld quality and heated area at 5-deg V angle.

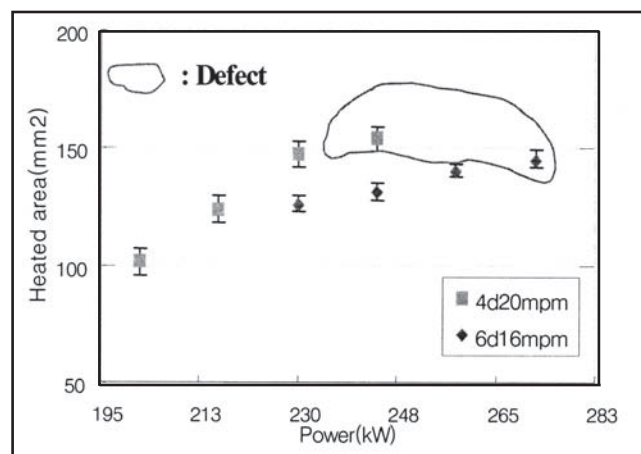


Fig. 14 — Relationship between weld quality and heated area at 4- and 6-deg V angle.

measured from the four lines obtained through images taken in 0.001-s intervals. The '5d16mpm' in the figure denotes that the V angle is 5 deg and the welding speed is 16 m/min. Each point shows the mean value of the heated width, and the fluctuation of the heated width is expressed through the standard deviation. The heated width has a tendency to increase as the welding power increases in all areas. The fluctuation shown in the figure through the standard deviation, however, is quite large under all welding conditions, showing that the heated width is not a suitable factor to express the heat input in quantitative terms.

Figure 11 shows the heated width measured from the image taken in 0.1-s intervals. The images taken in 0.1-s intervals also show that the heat width has a tendency to increase as the welding power increases similar to the images taken in 0.001-s intervals. However, the fluctuation under each welding condition is too great

to express the welding phenomenon in quantitative terms.

Figure 12 shows the changes in the heated area obtained through the images taken in 0.001- and 0.1-s intervals. The heated area was the gray level of area exceeding 110 and was calculated by searching the area 10 mm above and below the V-convergence point and 20 mm to each side. The figure demonstrates that the heated area shows a linear increase as the welding heat input increases, and the fluctuation in the heated area under each condition has greatly decreased compared to the ones shown in Figs. 10 and 11. Table 2 shows the coefficients of variation for image data sampled per 0.1 s. The coefficient of variation is computed as (standard deviation/average)100, and it expresses the unexplained variability remaining in the data relative to the average response. The heated area of the workpiece, therefore, is concluded to produce a more accurate quantitative evaluation of the weld-

ing quality than previous weld quality monitoring and control system based upon the heated width. The reason for the heated area losing its linearity when the welding speed is 16 m/min and welding power is 244 kW is because the heated melting area is blocked due to the top roller. Figure 12 shows that the welding phenomenon can be observed through a standard 30 fps camera when using the heated area to evaluate the welding quality, making it possible to develop a cost-effective welding system in the production line based upon image processing.

X-ray and ultrasonic tests are conducted in order to identify the correlation between the weld quality and the heated area of the workpiece measured from the image. Figure 13 shows the correlation between the heated area obtained from the image taken when the V angle is 5 deg and the results of the nondestructive test. The conditions where defects have been discovered are marked. The regions within

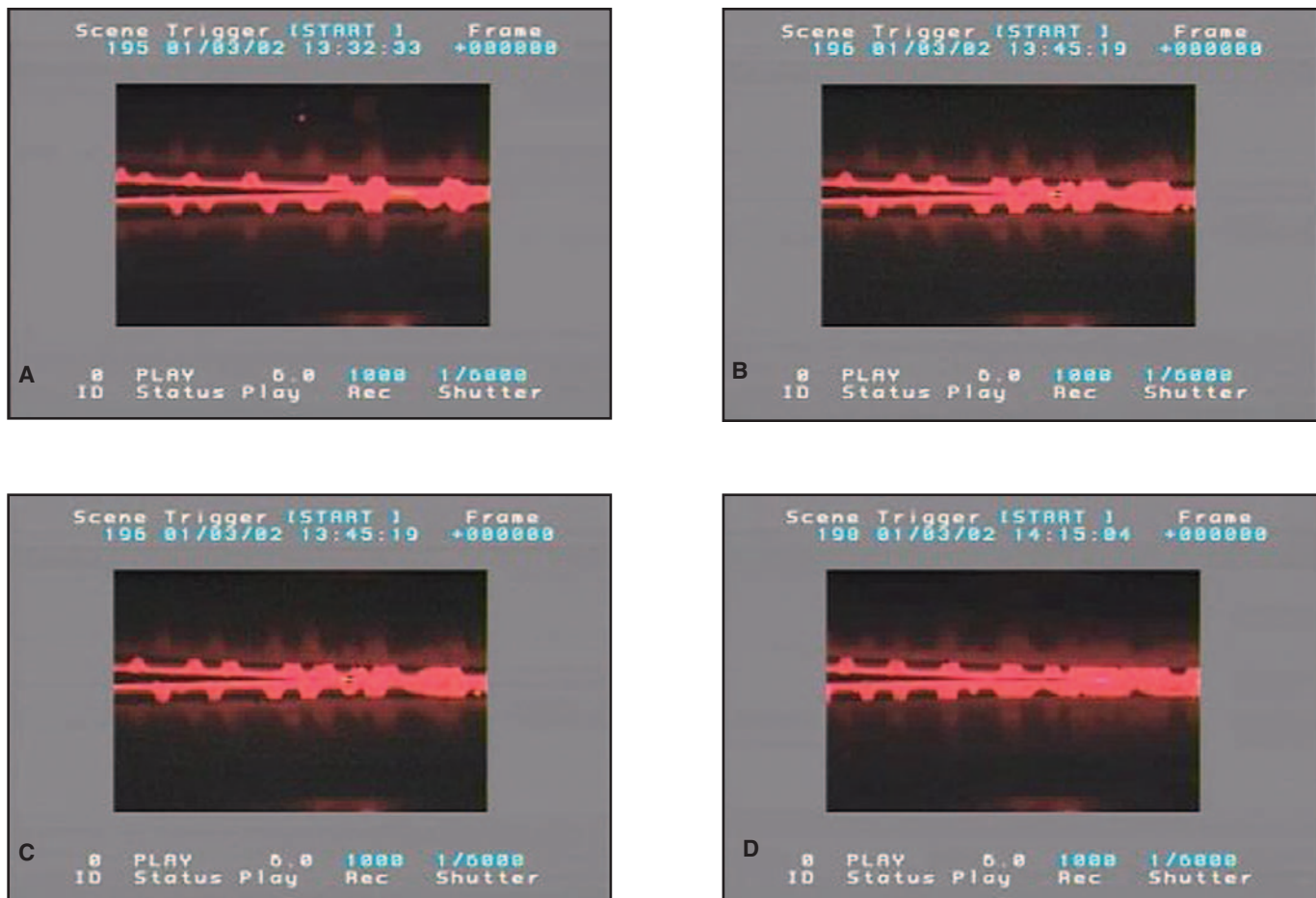


Fig. 15 — Effect of top roller on heated area at various welding powers. A — Welding power = 230 kW; B — welding power = 238 kW; C — welding power = 267 kW; and D — welding power = 285 kW.

the image where the heated areas are small are the areas where the heat input is low, causing weld defects. The regions within the image where the heated area is large are the areas where the heat input is also large, causing weld defects from excessive heat input. As seen from the results of studies published by Haga (Ref. 3), weld defects are equally found when the heat input is too small or too large. Cold weld, one representative weld defect in ERW, is found when the heat input is too small. Penetrator, another representative weld defect in ERW, is found when the heat input is too large. In particular, penetrators occur periodically along the weld seam. An optimal heat area is also shown to exist just as an optimal welding input exists, and thus the weld quality can be estimated through the heated area. The welded joint with 10 mm thickness used in this study display satisfactory weld quality, which don't show any weld defect in the nondestructive test when the heated area

is 100~150 mm², but display weld defects outside the heated area. Hence, it is possible to monitor weld defects by establishing a standard heated area and acceptable limits according to the material and the thickness of the workpiece.

The correlation between the heated area and weld quality obtained through the procedures above are applied to the image data captured while differing the welding power when the V angle is 4 and 6 deg. The relationship between the heated area measured from the image of the welding area and the weld quality is shown in Fig. 14. The heat area when the V angle is 4 and 6 deg shows a tendency to increase as the welding power increases similar to Fig. 13 where the V angle is 5 deg. Weld defects are also shown to occur under welding conditions where the heated area exceeds 150 mm². When the V angle is 6 deg, weld defects can be found where the heated area is less than 150 mm² because the top roller decreases the

heated area of the workpiece as seen in Fig. 15. If the top roller, which is a device used in the ERW simulator, does not prevent heat metal from flowing freely, the actual heated area would be measured at a larger value. Figure 15 shows several images captured under welding conditions wherein the V angle is 6 deg. The figure shows that there are more heated areas, which cannot be measured due to the top roller, as the welding power increases, bringing up the heat. It is, in addition, possible to generate an accurate measurement of the heated area by mechanically modifying the location of the top roller.

Based upon the method above, the heated area surrounding the V-convergence point is measured according to the material and thickness of the workpiece when welding steel pipes through HF-ERW. It is possible to monitor the weld quality during the welding process by comparing this value with the preset standard.

Conclusion

In high-frequency electric resistance welding (HF-ERW), the welding phenomenon surrounding the V-convergence greatly influences the weld quality. In this study, image data of the V-convergence point proximity are used in order to estimate the weld quality. The heated area is used as the parameter to evaluate the weld quality, and an optimal heated area is discovered just as an optimal heat input is found. Weld defects, which can be found when the heat input is too small, are discovered when the heated area is smaller than the optimal heated area. Weld defects, which occur under excess heat input, are also found when the heated area is larger than the optimal

area. Hence, the estimation of the weld quality is determined possible in this study through heated area.

References

1. O'Brien, R. L., ed. 1991. Welding process. *Welding Handbook*, 8th Ed., Vol. 2, pp. 652-669. Miami, Fla.: American Welding Society.
2. Haga, H., Aoki, K., and Sato, T. 1980. Welding phenomena and welding mechanisms in high-frequency electric resistance welding-1st report. *Welding Journal* 59(7): 208-s to 212-s.
3. Haga, H., Aoki, K., and Sato, T. 1981. The mechanisms of formation of weld defects in high-frequency electric resistance welding. *Welding Journal* 60(6): 104-s to 109-s.
4. Watanabe, N., Funake, M., Sanmiya, S., Kosuge, N., Haga, H., and Mizuhashi, N. 1986. An automatic power input control system in high-speed frequency electric resistance weld-

ing. *Transactions ISIJ* 26: 453-460.

5. Mihara, Y., Suzuki, K., Ohkawa, T., Harada, N., Komine, I., and Ishiro, S. 1986. A new automatic heat input control for production of electric resistance welded pipe. *Transactions ISIJ* 26: 476-483.

6. Tatsuwaki, M., Takamadate, C., and Hotta, K. 1984. Temperature pattern measurement and weld control in electric resistance welded tube mill. *Transactions ISIJ* 24: 847-856.

7. National Instruments Corp., LabVIEW version for Windows™, 2000 edition.

JOM-14
Fourteenth International Conference
On the Joining of Materials
&
The 5th International Conference on
Education in Welding
April 29–May 2, 2007
Helsingør, Denmark

The conference begins with registration on Sunday, April 29, 2007. Monday will mark the opening of eight sessions of presentations through Wednesday, May 2. AWS President Gerald Utrachi will make an opening address to attendees, as well as chair one of the sessions and make a technical presentation. A sampling of the topics that will be covered during the three days include the following:

- Mechanical properties and microstructure of ultra high-strength steel
- Metal powder laser deposition
- Improving weld joints in oil and gas pipelines
- Microbiological induced corrosion
- Hybrid laser welding of pipe
- Keyhole plasma arc welding
- Vision systems for arc welding
- Friction stir welding
- Welding dual-phase steel
- Metal transfer behavior
- Submerged arc welding optimization
- Solid-state welding
- Resistance spot welding parameters
- e-learning for welding
- University welding education
- ISO standardization and certification
- Weld quality and gas waste in GMAW
- Education and research
- Modeling temperature distribution in pipe welding

For more information or conference registration contact JOM- Institute Gilleleje Strandvej 28. DK-3250 Gilleleje, Denmark; telephone: +45 48355458; e-mail jom_aws@post10.tele.dk.

WELDING *Journal*

Guidelines for submitting electronic files

1. Platform:

Macintosh or PC accepted

2. Files accepted:

QuarkXpress, Adobe Photoshop, Adobe Illustrator, TIFF, EPS and PDF files only.

3. Color:

Send all files in as CMYK (for color) or Grayscale (for b/w).

4. Images:

Minimum resolution required for magazine printing is 300 dpi for full color artwork or grayscale at least 1000 dpi for bitmap (B&W/line art). Images and logos from Web sites are NOT usable for printing. They are low resolution images (72 dpi). Images taken with a digital camera are not acceptable unless they meet the minimum 300 dpi requirement.

5. Proof:

A proof of the images should **always** be provided.

6. Electronic File Transfer:

Files larger than 68k are not acceptable as an email attachment; please send it on a CD or Zip, you may also send files to the printer FTP site (a user name and password will be provided when requested)

Check list for submitting electronic files:

Colors: 4/C Grayscale B&W/line art

File Type: TIFF EPS

File sent via: Floppy disk Zip disk CD Email

Proof supplied/faxed

CMYK images at 300 dpi or higher, B&W/line art at 1000 dpi or higher.

All color in all images set to CMYK process (not RGB)

When submitting ads, please send them to the attention of

Frank Wilson
Advertising Production Manager
American Welding Society
550 NW LeJeune Rd.
Miami, Fla. 33126